



Investigation of Clean Energy Production in Drinking Water Networks

Veli Süme¹ · Rasoul Daneshfaraz² · Ali Kerim¹ · Hamidreza Abbaszadeh³ · John Abraham⁴

Received: 15 August 2023 / Accepted: 10 January 2024 / Published online: 7 February 2024
© The Author(s) 2024

Abstract

Viable renewable energy sources must be low-cost, easy to install, clean, and reliable if they are to meet the energy demand of urban or rural areas. Water is able to provide efficient sources of electrical energy among alternative renewable energy sources. Using modern hydraulic techniques, drinking water can be transported to the areas where it is needed. Studies on obtaining energy from drinking water networks are quite limited. Although not as necessary as water in terms of human health, electrical power is still critically important in many applications (lighting, heating, cooling, etc.). Consequently, many countries are developing energy using various renewable energy sources. In this study, a water distribution network in the Armağan Village of Maçka district of Trabzon province were used to obtain electrical energy. There are 47 pressure breaking valves (PBVs) in this network and the broken energy height is 236.35 m. The same energy loss can be achieved by installing microturbines instead of PBVs, and electricity generation can thus be achieved with a clean energy source. It was found that 84.12kWh of energy was obtained from each PBV, with a total of 3950kWh. The most suitable microturbine was selected according to sound microturbine selection criteria. From this study, it is revealed that electricity can be produced by using a Microturbine instead of Pressure Breaker Valves (PBVs).

Keywords Renewable energy · Drinking water network · Pressure breaker valve (PBV) · Kaplan-Pelton Microturbine · Electricity generation

✉ Veli Süme
veli.sume@erdogan.edu.tr

¹ Department of Civil Engineering, Faculty of Engineering, Recep Tayyip Erdogan University, Rize, Turkey

² Department of Civil Engineering, Faculty of Engineering, University of Maragheh, Maragheh, Iran

³ Department of Water Engineering, Faculty of Civil Engineering, University of Tabriz, Tabriz, Iran

⁴ School of Engineering, University of St. Thomas, St. Paul, MN 33901, USA

1 Introduction

Increasing energy costs and climate change has left industrialized and industrializing countries in a difficult situation regarding their future energy sourcing. This situation has pushed countries to seek energy production from renewable energy sources. Producing electrical energy by utilizing the energy of water is potentially an economical and environmentally renewable energy source. It has been observed that a mere 1% increase in renewable energy usage leads to a consequential reduction in CO₂ emissions by 0.14% in the long run (Raihan et al. 2022). After the Paris Agreement was signed, many countries made a commitment to reduce their greenhouse gas emissions to combat climate change. This led to a greater focus on the need for clean energy sources with low carbon footprints. One clean energy source is hydropower, which has emerged as a popular and viable solution for generating electrical energy (Yazdi and Moridi 2018). Other research has been produced that deals with the preservation of the environment and the generation of energy (Abdelzahr 2021, 2022; Elkhoully et al. 2022; Abraham et al. 2022) and the cost–benefit analysis of various social actions.

Hydroelectric systems are systems that generate electrical energy by utilizing the energy of water. Microturbines are rotated with the kinetic energy generated ultimately by the potential energy of flowing water and electricity power is produced by the generator connected to the microturbines. In hydraulic microturbines, the speed and pressure of the water passing through the microturbine wheel converts the rotating microturbine shaft into mechanical energy. They can be divided into different classes according to operating modes, construction styles, water height (head), and the direction of the water flow in the shaft. Sometimes, hydraulic microturbines can be divided into high-pressure microturbines and free-jet microturbines. The microturbine outlet may be above atmospheric pressure, or it may be at a lower than atmospheric pressure to increase efficiency. In free-jet microturbines, the pressure coming into the microturbine and the pressure leaving the microturbine are equal to the atmospheric pressure. Here, the potential energy of the water is first converted into kinetic energy and then subsequently into mechanical energy.

The efficiency of microturbines is related to their design and they are designed according to head and flow. The specifics of the application affect which type of microturbine should be used where and are critical to the design of the entire microturbine system. Ogiyar and Vidal (2009) analyzed the costs for small scale hydropower, which are distributed among civil work (40%), microturbine (30%), electro-mechanical and regulation equipment (22%), and construction management (8%). Kosnik (2010) developed an economic analysis based on several small plants with a non-linear relationship between the cost of implementation and installed power (small, micro, or pico).

Energy recovery to harness the power dissipated by valves (in pressurized flows) or hydraulic jumps (in open channels) is becoming common in fluid distribution channels (Pérez-Sánchez et al. 2017; Daneshfaraz et al. 2022). The use of water microturbines instead of pressure-breaking valves (PBVs) or nozzles in water distribution networks generate energy in this way and reduce water losses. Thus, while PBVs reduce the pressure by reducing the energy, hydraulic microturbines also remove energy from the fluid. In other words, microturbines reduce the pressure in the water network and generate electricity.

Spänhoff (2014) performed a worldwide projection of the installed capacity of renewable energy for the United States Energy Information Administration. Hydropower was the largest renewable source of energy in the period 2004–2010, and it will probably have the highest installed capacity in 2035.

As mentioned earlier, the working principle of water microturbines is to convert the potential energy of the water first into kinetic energy and then the kinetic energy into mechanical energy and transfer it to the generator via the microturbine shaft. The shaft generates electrical energy by rotating the generator shaft. This generated energy can be connected to the electricity grid or stored for later use.

Williams (1996) carried out a research in Blackpool, England where small micro-turbine pumps (PAT—Pump as Microturbine) were used for hydroelectric production in water distribution networks. Fontana et al. (2012) conducted a similar study in Italy using micro-hydropower (MHP) technology in water pipelines and other water infrastructure. Potential of this application was also demonstrated by Gaius-obaseki (2010). At points of high excess pressure, energy may be recovered using MHP technology without interfering in the water supply service (McNabola et al. 2011). Corcoran et al. (2013) conducted studies on water distribution networks in Ireland and England. In the study where 95 potential areas were determined They calculated the annual energy produced with system efficiencies of 65%. Kaplan microturbine between Francis and fixed blade microturbines was the most efficient microturbine for a range of flow rates. McNabola et al. (2014) investigated the economic and technical aspects of energy production by using microturbines in water distribution networks together with drains in Ireland. They produced 13 kW of energy in a financially viable manner. They showed that 1350 tons of CO₂ emission savings can be achieved annually by using 10 nozzles and microturbines. Pérez-Sánchez et al. (2017) investigated hydraulic energy generation in drinking and irrigation water networks through an extensive review and analyzed the economic and environmental implications of large and small hydropower systems and how hydropower can be applied in water distribution networks.

Itani et al. (2020) investigated energy recovery using water turbines in water transmission pipelines. They simulated an existing water pipeline under several velocity scenarios. They showed that a large amount of energy can be recovered by installing Pelton turbines. Postacchini et al. (2020) conducted a laboratory investigation using a pump as a turbine. Their results confirm the good performance of the PAT system when the rotational speed and water demand are greater than 850 rpm and 8 l/s, respectively. Alnaqbi et al. (2022) investigated the application of hydropower generation and pumped hydro-power storage in the Middle East and North Africa. The results showed that in all the countries that have been investigated, pumped hydro storage (PHS) will play a central role in the stability of the energy supply and the adoption of renewable energies.

Energy is one of the most basic prerequisites for economic and social development of countries around the world. Demographic changes and urban growth have caused an increase in energy demand and rapid expansion in the consumption of resources. While the methods of energy supply and production are the determining factors for pollution, the rapid depletion of non-renewable energy sources and the increase in pollution have caused various environmental costs. Today, with increasing need for energy, new and small-scale energy sources should be evaluated. The review of the research background showed that no study has been performed on use of microturbines instead of pressure breakers. Microturbines reduce the water pressure and produce clean energy from low flow. The use of small hydroelectric facilities in water supply systems is preferred due to its low cost. Therefore, the current study focuses on the potential for using drinking water networks as a source of clean-energy production. This investigation improves the design of hydraulic control structures and protects the environment by producing clean and renewable energy.

2 Materials and Methods

Use of microturbines vary according to the size of the hydraulic head and the water flow passing through the microturbine. Selection of the microturbine depends on a variety of factors including the specific speed, the water flow rate to the microturbine, and the number of revolutions. In Fig. 1, the Kaplan microturbine and its structure, the diagram of the turbine, and the schematic view of the clean energy production are shown. Proper micro-turbine choice can improve overall efficiency of the system. The net head is obtained by subtracting the vertical distance from the water source to the microturbine from the hydraulic losses. These losses are due to friction and minor losses in the pipe, elbows, and valves.

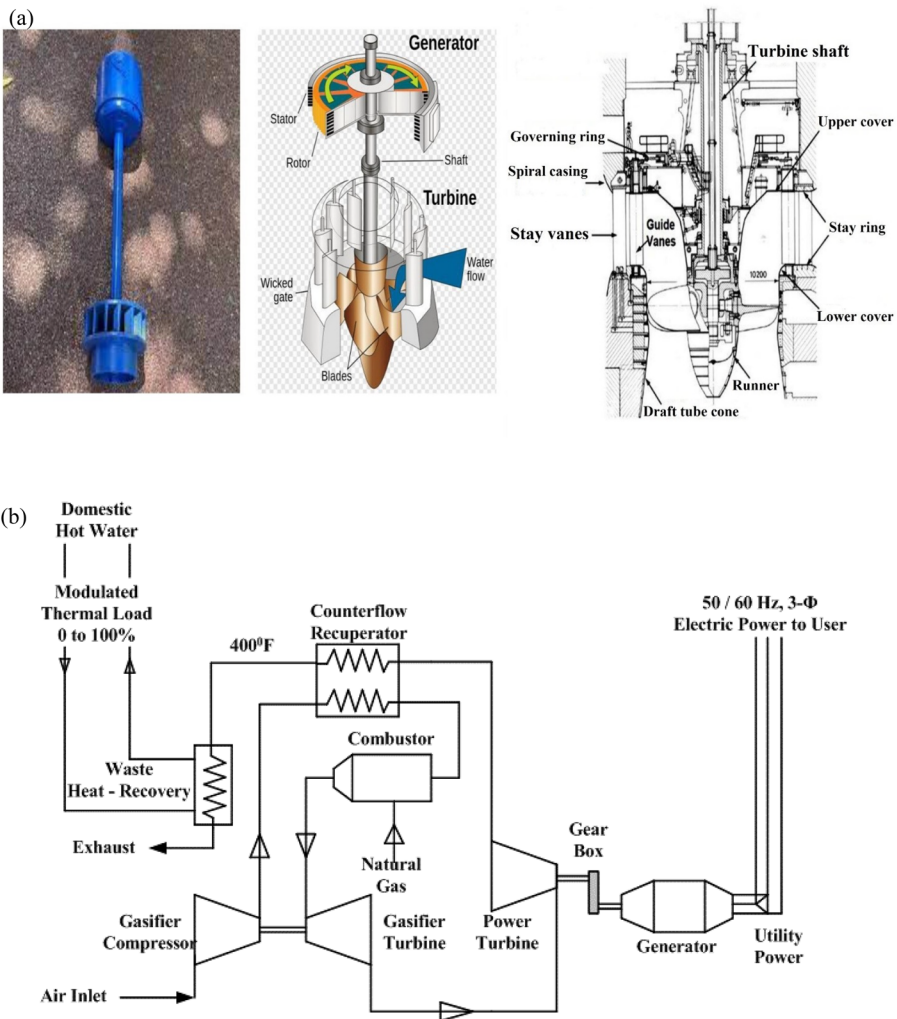


Fig. 1 The view of **a**) Kaplan microturbine structure (Topliceanu et al. 2016), **b**) diagram of Kaplan micro-turbine, **c**) clean energy production from drinking water network

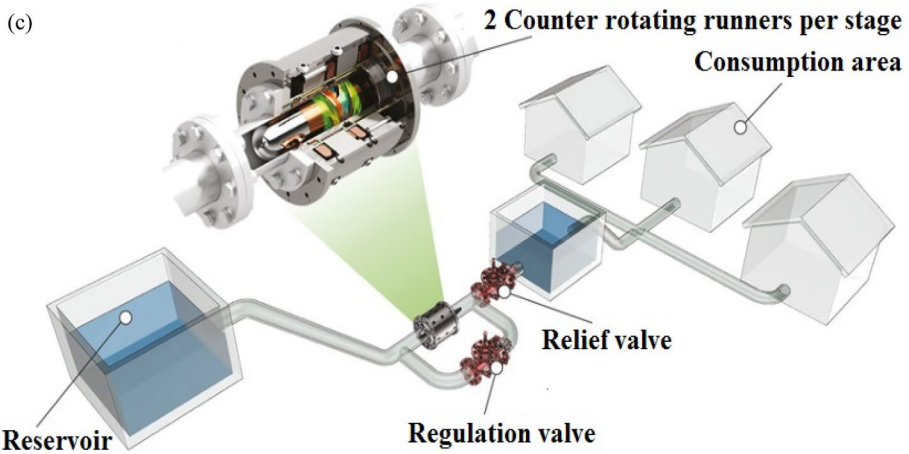


Fig. 1 (continued)

The energy equation is expressed as:

$$H = H_g - \Sigma\xi = H_g - (0.5 + k_1 + k_2 + k_3 + \lambda \frac{L}{D}) \frac{V^2}{2g} \tag{1}$$

In Eq. (1), H represents the net head, H_g the gross head, and $\Sigma\xi$ the total losses. The terms k_1, k_2, k_3 are the loss coefficients, λ is the friction coefficient, L is the pipe length, D is the pipe diameter, V is the velocity of the water and g is the gravitational acceleration. Figure 2 shows the schematic representation of the flow system and various nomenclature.

The volumetric flow rate is calculated by:

$$Q = VA \tag{2}$$

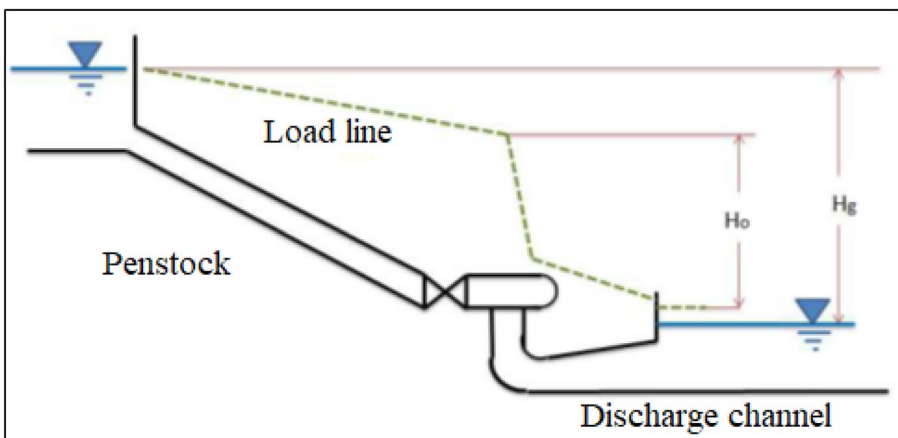


Fig. 2 Schematic representation of net-gross head

Here, Q is the volumetric flow rate (m^3/s), V is the water velocity (m/s), and A is the cross-sectional area (m^2).

The number of revolutions per minute required for a microturbine to produce 1 kW of power under 1 m head is called the specific velocity of the microturbine and will be denoted by n_s later in this manuscript. Specific velocity, which is an important parameter in determining the most suitable microturbine type, is frequently used in hydraulic machines; the specific velocity is determined by the flow and head parameters.

"Drinking, Utilization, Industrial Water Supply, and Distribution Network Project Construction Work", which was produced in 2020 by Trabzon Drinking Water and Sewerage Administration (TDWSA) is affiliated with Trabzon Metropolitan Municipality. The project was made by the Karakaya Group. The energy potential of the current drinking water network lines was evaluated according to the flow rates and the incoming and outgoing pressures of the PBVs without making any changes on the line. Microturbine selection criteria were applied according to the head flow and specific velocity.

Only the network lines covering the 1st region main storage basin were used by the Karakaya Group Drinking Water application project. This portion is located in the Armağan Village of Maçka district of Trabzon province.

Maslak was not used in the study area as the field conditions were not favorable, and a proportional pressure breaker valve was used in the entire network. In addition, a parallel line to the main line is planned before each pressure breaker valve so that the pressure did not fall below 30 m.

In the project, 48 PBVs were utilized and one PBV was excluded from the study because the data in the calculation table and the plan were incompatible. Therefore, a study was conducted with 47 PBVs. The area is approximately 15 km away from Trabzon city center and a Google Earth satellite image of the network line is given in Fig. 3. Figure 3 shows the distributions of PPV in the plan.

Microturbine selection criteria were applied for electricity generation in drinking water network lines. First, a microturbine selection was made based on both the head and flow rate. These data were taken from the 1st Region Main Storage Network Calculation Table in the Karakaya Group Drinking Water Project (Table 1). In Fig. 4, microturbines used in hydroelectric facilities with different head and flow regions are shown.

For the head values, the pressure differences with the pressure at the PBVs are expressed as Net Head. This enables the pressure damped in PBVs to be used in energy generation. The discharge data for each pressure breaker valve are provided in Fig. 5. The highest flow data occurred was $0.01134 \text{ m}^3/\text{s}$ PBV4 and the lowest at $0.00104 \text{ m}^3/\text{s}$ occurred at PBV23.

The velocity data for each pressure breaker valve (PBV) are shown in Fig. 6. Head height decreases where velocity increases. As seen in Fig. 6, the maximum velocity is $0.9663 \text{ m}/\text{s}$ at pressure breaker valve 25 (PBV25) and the minimum velocity is $0.4259 \text{ m}/\text{s}$ at pressure breaker valve 18 (BV18). As in Fig. 7, it is seen that the pressures at the inlets to the pressure breaker valve (PBV) are large, while the pressure values at the outlets are low. The maximum pressure head 64.49 m before pressure breaker valve 4 (PBV4). After PBV4, the pressure head is 22.93 m . The relative pressure elevation change was 64.44% . The minimum pressure height is 37.02 m before PBV27 while after PBV27 it is 12.77 m . and the relative change percentage is 65.5% . In Fig. 8, the absolute head change is given for each PBV. As seen in Fig. 8, at PBV27 the maximum absolute pressure decrease is 24.25 m .

To calculate the specific velocities at each PBV, the gross power must be calculated and the microturbine velocity must be determined. Gross power can be calculated according to Eq. (3) using the data in Table 1 and there are various energy losses that occur inside the microturbine and can be expressed with power P_0 .

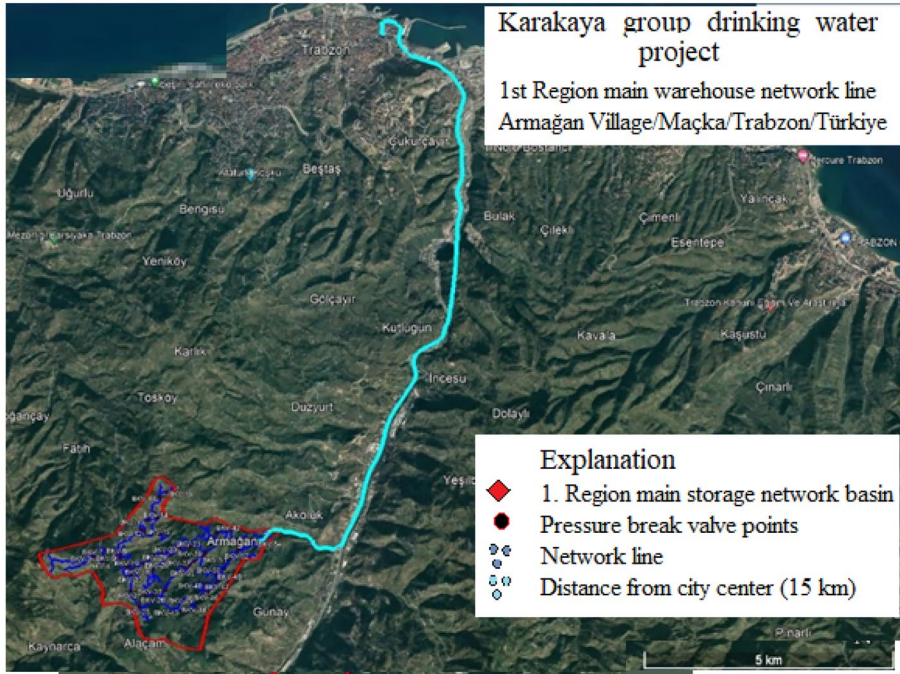


Fig. 3 Google Earth satellite image showing the study area

Table 1 Microturbine types by Specific velocity (n_s), Efficiency (%) and Head (m)

Microturbine Types	Specific velocity (n_s) (rpm)	Efficiency η_t (%)	Head height (m)
Pelton (single nozzle)	0.5–36	89	350–1800
Pelton (dual nozzles)	36–85	90	
Francis	3.8–500	94	64–700
Kaplan	17.2–1200	93	6–50
Banki (Cross Flow)	10–130	74.5	2–150
Turgo	3–70	70	400–600

$$P_0 = \frac{Q \cdot \rho \cdot g \cdot H}{10^3} \tag{3}$$

In Eq. (3), P_0 is the power extracted from the microturbine shaft (kW), Q is the flow rate to the microturbine (m^3/s), ρ is the density of water ($\approx 1000 \text{ kg/m}^3$), g is the gravitational acceleration ($9.81 \text{ m}^2/s$), H is the net head (m). Microturbine selections were determined from Table 1 according to the specific velocity values given in Eqs. (4–8).

The turbine rated velocity in rpm is represented by n_s . It has been formulated and brought to the literature with work by different researchers in Türkiye.

For n_s , the microturbine types according to Siervo and Leva are determined from Table 1 using:

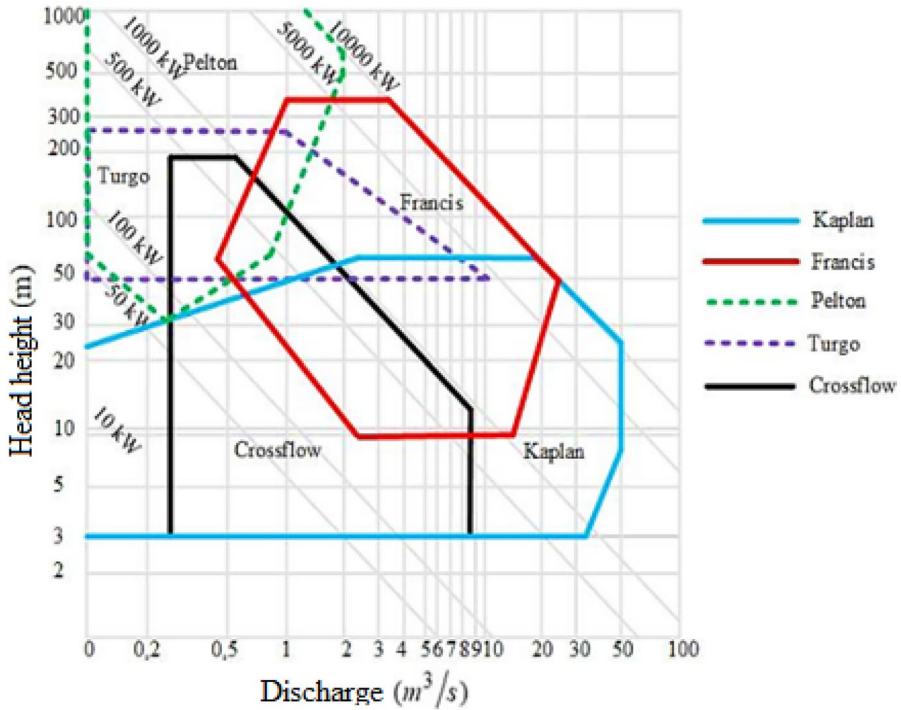


Fig. 4 Types of microturbines to be used according to flow and head values (up to 10 MW)

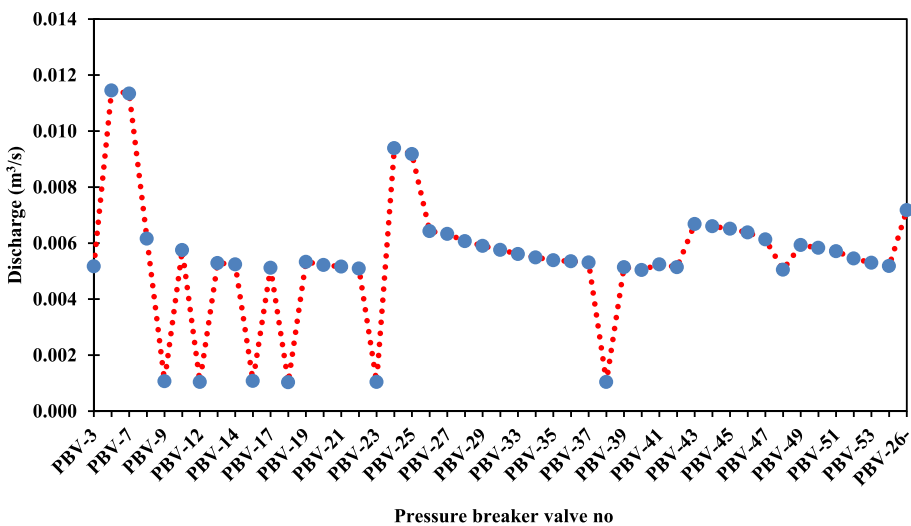


Fig. 5 Pressure breaker valve-discharge

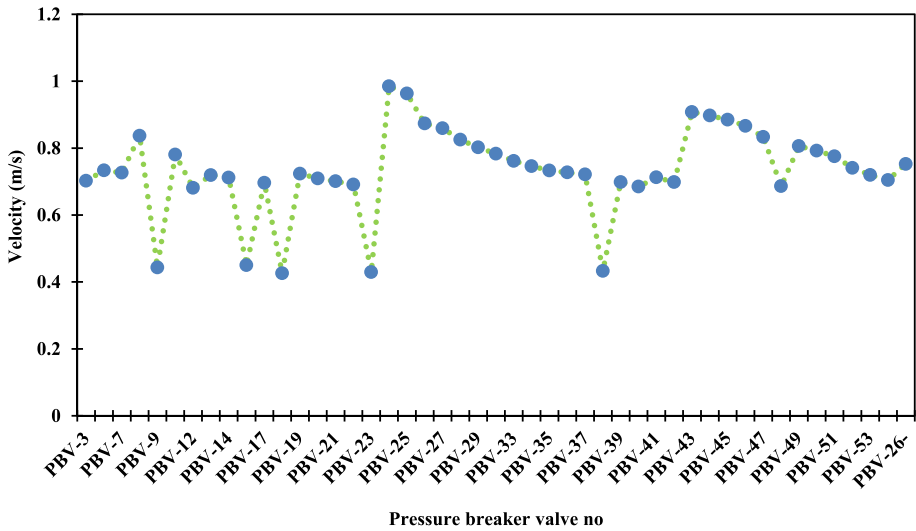


Fig. 6 Pressure breaker valve-velocity

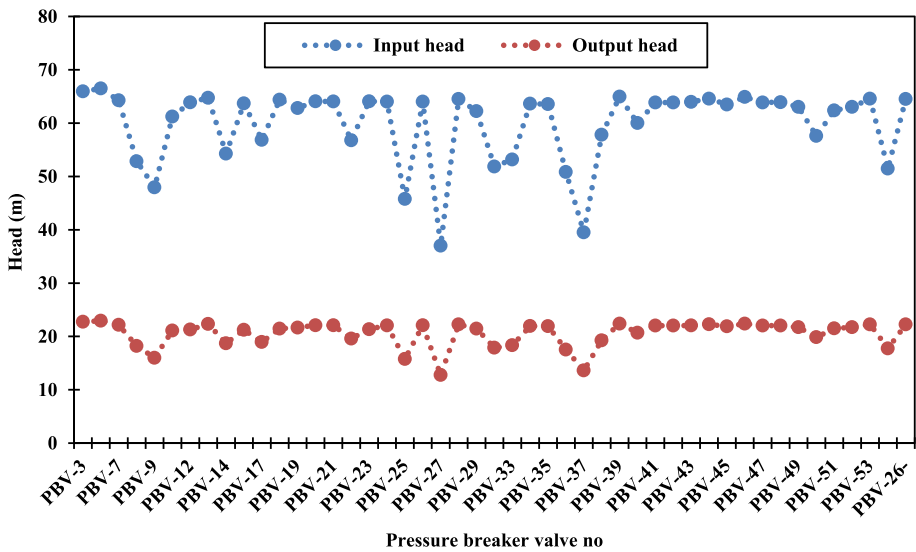


Fig. 7 Pressure breaker valve-head

$$n_s = \frac{3470}{(H)^{0.65}} \text{ (rpm)} \tag{4}$$

In Eq. (5), microturbine types are determined from Table 1, from:

$$n_s = n \frac{\sqrt{P_0 \times 1.358}}{(H)^{1.25}} \text{ (rpm)} \tag{5}$$

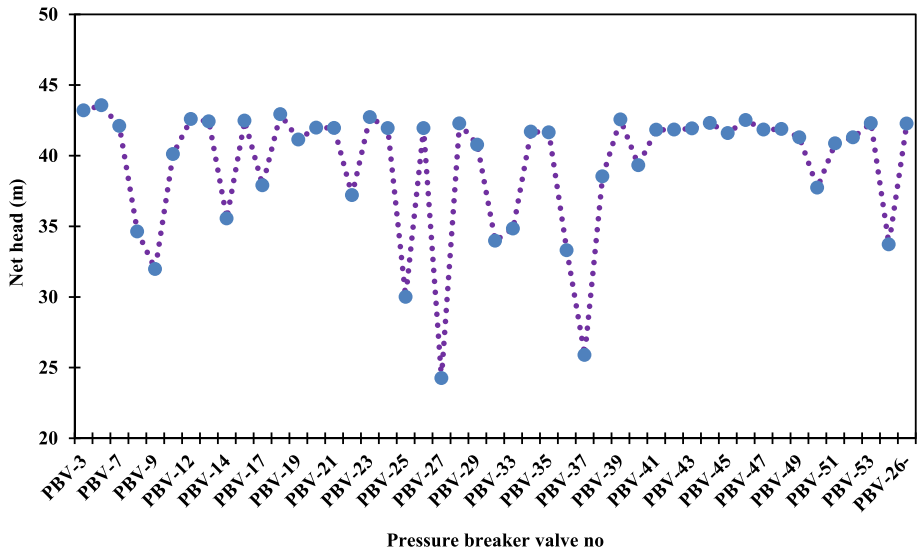


Fig. 8 Pressure breaker valve-net head

In Eq. (6), microturbine types are determined from Table 1, according to:

$$n_s = n \frac{\sqrt{\frac{P_0}{\rho}}}{(gH)^{1.25}} \text{ (rpm)} \tag{6}$$

In Eq. (7), microturbine types are determined from Table 1 and is based on:

$$n_s = n \frac{\sqrt{Q}}{H^{0.75}} \text{ (rpm)} \tag{7}$$

In Eq. (8), from Demirhan, (2006), microturbine types were determined from Table 1, as

$$n_s = n \frac{\sqrt{P_0}}{H^{1.25}} \text{ (rpm)} \tag{8}$$

In Eqs. (4-8); n_s is the specific velocity of the microturbine (rpm), n is the rated velocity of the microturbine (rpm), P_0 is the microturbine gross power (kW), H is the net head (m), ρ is the density of water, g is the gravitational acceleration, and n_s is the specific velocity. Most of these terms have already been defined. When the rotation velocity is taken into account using units of rpm, the outcome is unitless. When the rotation velocity is taken in terms of rad/s, the output units are in radians.

In Table 1, n_s turbine rated velocities in the 2nd column are the results found with Eqs. (4-8) and which shows the value ranges. The efficiency of the microturbine based on the type of microturbine. The ratio of the power taken from the microturbine to the supplied power is called the overall efficiency. It is expressed with η_r . Microturbine efficiency depends on the flow rate.

Generator selection was made according to gross power, head, flow rate and the micro-turbines (Table 1). The efficiency of the generator is 0.94.

The amount of electrical energy obtained, the net head height, the flow rates in the network, and the microturbine and generator type data suitable for these flows are listed in Table 2.

The aim of this study is to obtain maximum energy with a minimum discharge rate. Because the discharge rates in the city networks are generally low. Therefore, when Table 2 is examined, it is seen that the most appropriate discharge data is 0.005–0.028 m³/s and the maximum energy is obtained at this discharge. In other words, the highest energy can be obtained at the lowest discharge value. So the necessity of using the Pelton microturbine and Asynchronous Generator, where the pressure difference is between 12–34 m, emerges.

3 Results and Discussions

3.1 Microturbine Selection in the Network Line

The initial phase of microturbine selection involved a meticulous analysis based on the parameters outlined in the calculation table, as presented in Table 2. The criteria for selection were derived from the head-flow rate graph, illustrated in Fig. 4, taking into account the specific velocity equations (Eqs. 4–8). In this process, the microturbine efficiencies, essential for the subsequent steps, were compiled in Table 3. Upon evaluating the flow rates, which ranged from 0.00103 m³/s to 0.01145 m³/s, and the net heights of the pressure breaker valve (PBV) within the range of 24.25 to 43.56 m, it became evident that both Pelton and Kaplan microturbines were viable alternatives for replacing each PBV. Following the microturbine selection phase, the subsequent step involved the careful consideration of generator specifications. The generators were chosen in alignment with the identified microturbines that met the selection criteria, as delineated in Table 3. The culmination of this process is encapsulated in the net power calculations, detailed in Table 4, which accounts for factors such as generator velocity and efficiency. This systematic approach ensures the integration of the chosen microturbines and generators in a manner that optimizes net power output, incorporating head-flow rates, specific velocities, and overall system efficiency.

Subsequent to the assessment of rated velocity, the decision-making process advanced with the utilization of Eqs. (4–8) to determine specific rated velocity (n_s) values. This numerical quantification played a pivotal role in refining the selection criteria, adding a

Table 2 Power obtained according to microturbine types in the drinking water network

Power (kW)	Net height (m) (Min–Max)	Discharge (m ³ /s) (Min–Max)	Turbin-Generator
0.2–1	1.5 max	0.05–0.13	Kaplan; Permanent Magnet AA Generator
0.3–5	2–5	0.028–0.12	Kaplan; Asenkron Generator
0.2–0.5	5–12	0.006–0.01	Turgo; Permanent Magnet AA Generator
0.6–2	8–17	0.02–0.03	Turgo; Asenkron Generator
0.3–5.5	12–34	0.005–0.028	Pelton; Asenkron Generator
5–8	24–34	0.033–0.04	Turgo; Senkron Generator
9–16	24–34	0.066–0.08	Pelton; Senkron Generator
1.5–5	30–90	0.008–0.03	Pelton; Senkron-Asenkron Generator

Table 3 Microturbines in the study area (Low-Flow Rate)

PBV	Discharge Q (m ³ /s)	Net Pressure H (m)	Turbine Types	PBV	Discharge Q (m ³ /s)	Net Pressure H (m)	Turbine Types
PBV-3	0.00517	43.20	Pelton-Kaplan	PBV-33	0.00561	34.84	Pelton-Kaplan
PBV-4	0.01145	43.56	Pelton-Kaplan	PBV-34	0.00549	41.70	Pelton-Kaplan
PBV-7	0.01134	42.10	Pelton-Kaplan	PBV-35	0.00539	41.64	Pelton-Kaplan
PBV-8	0.00616	34.63	Pelton-Kaplan	PBV-36	0.00535	33.30	Pelton-Kaplan
PBV-9	0.00107	31.97	Pelton-Kaplan	PBV-37	0.00531	25.89	Pelton-Kaplan
PBV-11	0.00575	40.11	Pelton-Kaplan	PBV-38	0.00104	38.53	Pelton-Kaplan
PBV-12	0.00104	42.59	Pelton-Kaplan	PBV-39	0.00514	42.56	Pelton-Kaplan
PBV-13	0.00529	42.42	Pelton-Kaplan	PBV-40	0.00504	39.32	Pelton-Kaplan
PBV-14	0.00524	35.55	Pelton-Kaplan	PBV-41	0.00524	41.83	Pelton-Kaplan
PBV-15	0.00108	42.47	Pelton-Kaplan	PBV-42	0.00514	41.84	Pelton-Kaplan
PBV-17	0.00512	37.90	Pelton-Kaplan	PBV-43	0.00668	41.92	Pelton-Kaplan
PBV-18	0.00103	42.93	Pelton-Kaplan	PBV-44	0.00660	42.31	Pelton-Kaplan
PBV-19	0.00533	41.14	Pelton-Kaplan	PBV-45	0.00651	41.59	Pelton-Kaplan
PBV-20	0.00522	41.98	Pelton-Kaplan	PBV-46	0.00638	42.52	Pelton-Kaplan
PBV-21	0.00516	41.96	Pelton-Kaplan	PBV-47	0.00613	41.84	Pelton-Kaplan
PBV-22	0.00509	37.20	Pelton-Kaplan	PBV-48	0.00505	41.88	Pelton-Kaplan
PBV-23	0.00104	42.72	Pelton-Kaplan	PBV-49	0.00593	41.29	Pelton-Kaplan
PBV-24	0.00939	41.94	Pelton-Kaplan	PBV-50	0.00583	37.73	Pelton-Kaplan
PBV-25	0.00918	30.00	Pelton-Kaplan	PBV-51	0.00571	40.87	Pelton-Kaplan
PBV-26	0.00643	41.94	Pelton-Kaplan	PBV-52	0.00545	41.29	Pelton-Kaplan
PBV-27	0.00633	24.25	Pelton-Kaplan	PBV-53	0.00530	42.30	Pelton-Kaplan
PBV-28	0.00607	42.28	Pelton-Kaplan	PBV-54	0.00518	33.72	Pelton-Kaplan
PBV-29	0.00590	40.77	Pelton-Kaplan	PBV-56	0.00718	42.27	Pelton-Kaplan
PBV-30	0.00576	33.97	Pelton-Kaplan				

precise dimension to the evaluation of microturbine performance. Simultaneously, power calculations were conducted in accordance with Eq. (3), adding another layer of insight into the overall system performance. The outcomes of these calculations have been systematically organized in Table 4, offering a comprehensive overview of the gross power values associated with each specific PBV point. This tabulated representation facilitates a comparative analysis of potential power outputs under diverse operational conditions, contributing to a holistic understanding of the microturbine system's capabilities.

Microturbines that can be selected according to the head-flow rate and specific velocities are given in Table 4 and Table 5. After the microturbine determination process was completed, the efficiency values should be determined. Efficiency values are selected according to the maximum microturbine efficiency of the microturbines that were used. For the Pelton 1 (one) nozzle microturbine, this value is 89% (Table 5).

In the generator selection, power, head and flow parameters were selected according to the Pelton Microturbine (Table 5). Considering these values, the generator that can be selected for the Pelton microturbine is the asynchronous type. Generator efficiency was taken to be 95%. In this context, net power was calculated according to the generator's velocity and efficiency. In Table 5, net power is a product of P , turbine rated velocity (η_t), and generator rated velocity (η_g), ($\eta_t=0.89$, $\eta_g=0.95$).

Table 4 Calculated specific velocity for microturbine selections

PBV	Power P (kW)	Turbine Rotate number n	Specific Velocity (rpm)				
			n_s (4)	n_s (5)	n_s (6)	n_s (7)	n_s (8)
PBV-3	2.19	1500	300.10	23.36	0.04	6.40	20.05
PBV-4	4.89	1500	298.48	34.55	0.05	9.47	29.65
PBV-7	4.68	1500	305.17	35.28	0.06	9.66	30.27
PBV-8	2.09	1500	346.49	30.10	0.05	8.25	25.83
PBV-9	0.34	1500	364.96	13.32	0.02	3.65	11.43
PBV-11	2.26	1500	314.93	26.05	0.04	7.14	22.35
PBV-12	0.43	1500	302.89	10.59	0.02	2.90	9.09
PBV-13	2.20	1500	303.67	23.96	0.04	6.56	20.56
PBV-14	1.83	1500	340.63	27.22	0.04	7.46	23.36
PBV-15	0.45	1500	303.44	10.81	0.02	2.96	9.28
PBV-17	1.90	1500	326.75	25.65	0.04	7.03	22.01
PBV-18	0.43	1500	301.32	10.48	0.02	2.87	8.99
PBV-19	2.15	1500	309.78	24.61	0.04	6.74	21.12
PBV-20	2.15	1500	305.74	23.98	0.04	6.57	20.58
PBV-21	2.12	1500	305.83	23.85	0.04	6.54	20.47
PBV-22	1.86	1500	330.73	25.93	0.04	7.10	22.25
PBV-23	0.44	1500	302.29	10.57	0.02	2.89	9.07
PBV-24	3.86	1500	305.93	32.19	0.05	8.82	27.62
PBV-25	2.70	1500	380.37	40.92	0.06	11.21	35.12
PBV-26	2.65	1500	305.93	26.64	0.04	7.30	22.86
PBV-27	1.51	1500	436.78	39.86	0.06	10.92	34.21
PBV-28	2.52	1500	304.33	25.73	0.04	7.05	22.08
PBV-29	2.36	1500	311.61	26.06	0.04	7.14	22.37
PBV-30	1.92	1500	350.85	29.53	0.05	8.09	25.34
PBV-33	1.92	1500	345.13	28.60	0.04	7.83	24.54
PBV-34	2.25	1500	307.07	24.72	0.04	6.77	21.21
PBV-35	2.20	1500	307.36	24.52	0.04	6.72	21.04
PBV-36	1.75	1500	355.42	28.89	0.05	7.91	24.79
PBV-37	1.35	1500	418.59	34.76	0.05	9.52	29.83
PBV-38	0.39	1500	323.27	11.42	0.02	3.13	9.80
PBV-39	2.15	1500	303.02	23.56	0.04	6.45	20.21
PBV-40	1.94	1500	319.03	24.75	0.04	6.78	21.24
PBV-41	2.15	1500	306.45	24.09	0.04	6.60	20.68

Upon careful examination of Figs. 9 and 10, a pattern emerges wherein the energy content exhibits a direct proportionality to both the pipe diameter and the flow rate. As the pipe diameter and flow rate increase, the energy content also experiences a corresponding increase. This correlation underscores the significance of these two parameters in influencing the overall energy dynamics within the system. Conversely, when the pipe diameter decreases while keeping the flow rate constant, there is a notable increase in the inlet pressure. This phenomenon reflects an inverse relationship between the pipe diameter and inlet

Table 5 Net power values at PBV points

PBV	Power P (kW)	Net Power $P_{\eta t, \eta g}$ (kW)	PBV	Power P (kW)	Net Power $P_{\eta t, \eta g}$ (kW)
PBV-3	2.19	1.852	PBV-33	1.916	1.623
PBV-4	4.894	4.134	PBV-34	2.246	1.902
PBV-7	4.685	3.957	PBV-35	2.203	1.86
PBV-8	2.093	1.767	PBV-36	1.748	1.48
PBV-9	0.335	0.287	PBV-37	1.348	1.141
PBV-11	2.261	1.911	PBV-38	0.394	0.33
PBV-12	0.433	0.364	PBV-39	2.146	1.818
PBV-13	2.203	1.86	PBV-40	1.944	1.64
PBV-14	1.827	1.547	PBV-41	2.152	1.818
PBV-15	0.452	0.38	PBV-42	2.109	1.784
PBV-17	1.905	1.606	PBV-43	2.747	2.325
PBV-18	0.432	0.364	PBV-44	2.74	2.317
PBV-19	2.149	1.818	PBV-45	2.657	2.249
PBV-20	2.15	1.818	PBV-46	2.66	2.249
PBV-21	2.123	1.792	PBV-47	2.517	2.131
PBV-22	1.856	1.573	PBV-48	2.075	1.75
PBV-23	0.434	0.372	PBV-49	2.403	2.029
PBV-24	3.864	3.264	PBV-50	2.158	1.826
PBV-25	2.703	2.283	PBV-51	2.288	1.936
PBV-26	2.645	2.241	PBV-52	2.209	1.869
PBV-27	1.505	1.277	PBV-53	2.198	1.86
PBV-28	2.519	2.131	PBV-54	1.715	1.446
PBV-29	2.361	1.995	PBV-26-	2.977	2.52
PBV-30	1.92	1.623			

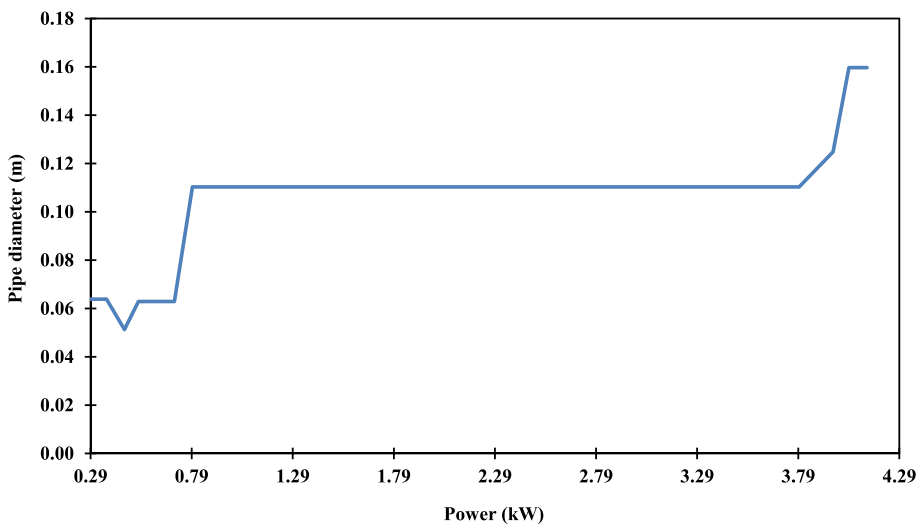


Fig. 9 Relationship between power and pipe diameter

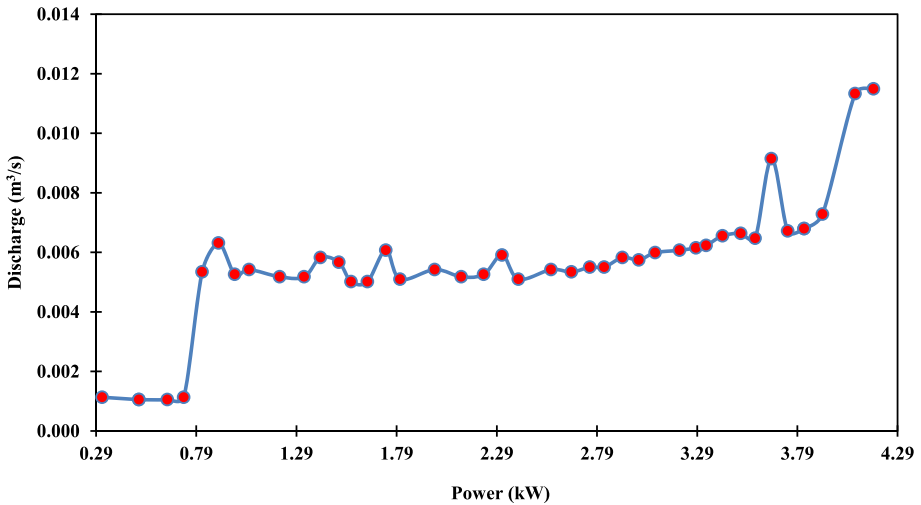


Fig. 10 Relationship between power and discharge

pressure. A reduction in pipe diameter results in elevated velocity and, consequently, an augmented net pressure. This, in turn, leads to a notable increase in the amount of energy obtained, as illustrated in Fig. 9. Analyzing the observed energy variations, it becomes apparent that microturbines characterized by lower rotational turbine rated velocity (n_s), may be preferred. The rationale behind this preference lies in the ability of microturbines with lower n_s values to effectively harness the increased energy generated by the system's dynamic conditions. In practical terms, the insights derived from Figs. 9 and 10 contribute to the strategic selection of microturbines based on the nuanced interplay between pipe diameter, flow rate, and energy outcomes. Opting for microturbines with a lower rotational turbine rated velocity aligns with the objective of optimizing energy extraction under varying operational scenarios. This consideration underscores the importance of tailoring microturbine selection to the specific dynamics of the fluid system, ensuring efficiency and performance in the decision-making process.

For each of the 47 PBVs, microturbine selection criteria were applied and it was concluded that Pelton microturbine was superior based on 6 parameters (Drop-Flow, n_s (Eq. 4), n_s (Eq. 5), n_s (Eq. 6), n_s (Eq. 7), and n_s (Eq. 8)). The specific velocities given in the ns (Eq. 4) and ns (Eq. 6) are incompatible with the other parameters, and the Low-Flow and n_s values from Eqs. (5, 7, and 8) are related to each other.

In Figs. 9, 10, 11, 12, and 13, the relations of water flow, water velocity, pipe diameters, net head, operating pressure, and the specific velocities n_s (Eqs. 5, 7, and 8) are related to each other according to the calculated net power. In Figs. 9, 10, and 12, when the net power exceeds 0.38 kW, there is a sudden change in the water flow rate, water velocity, and pipe diameters. Figures 11 and 13 shows specific velocities (Eqs. 5, 7, and 8) in a random distribution in the graph of operating pressure and net head.

The present research offers a detailed microturbine selection process, considering specific velocity equations and providing a systematic approach to optimize net power output. The inclusion of generator specifications and a comprehensive analysis of energy dynamics sets it apart. In contrast, Corcoran et al. (2013) and McNabola et al. (2014) focus on energy production, with less emphasis on the nuanced interplay of parameters observed in the present study.

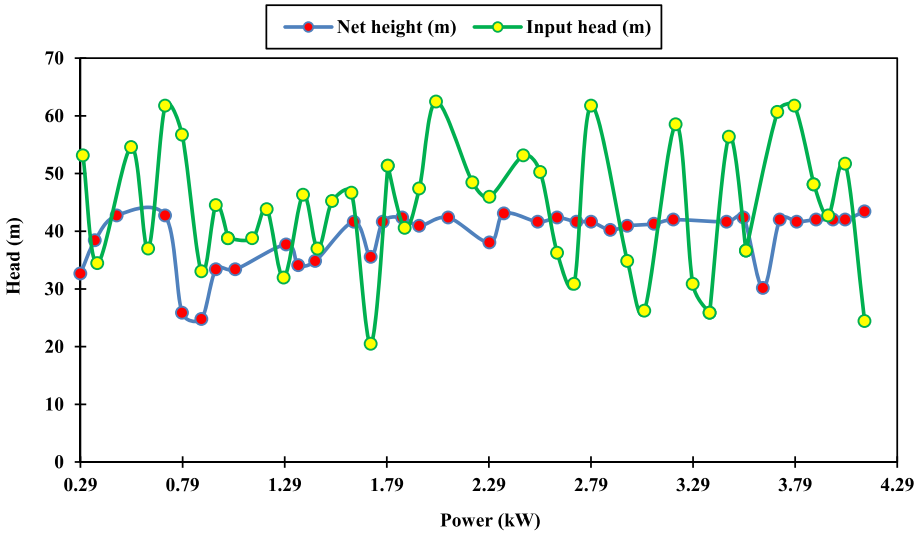


Fig. 11 Relationship between head and power

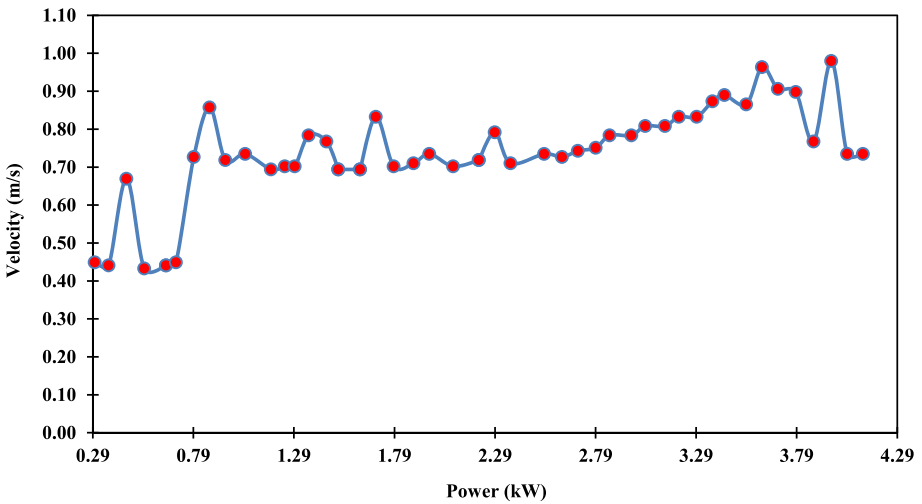


Fig. 12 Relationship between power and velocity

The strategic microturbine selection criteria and the detailed exploration of energy outcomes under diverse conditions distinguish the present article as a more intricate and methodologically robust study.

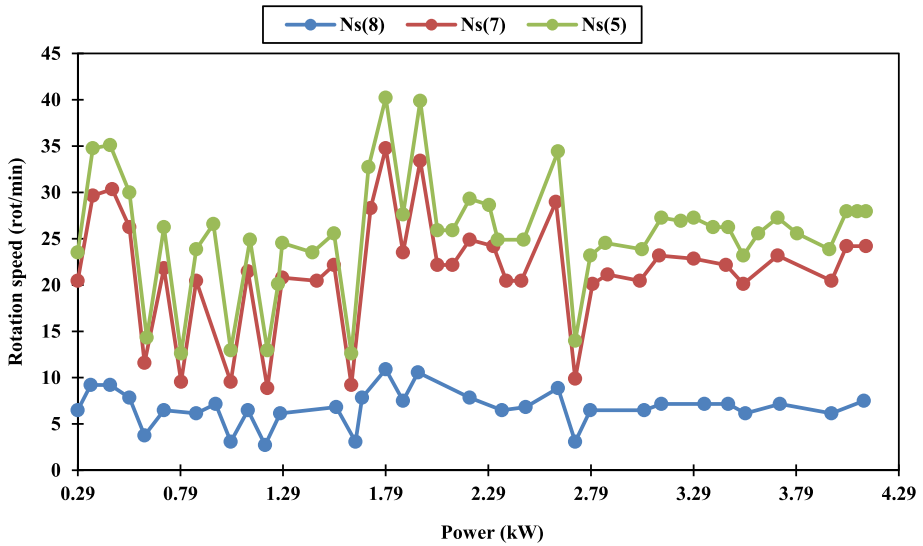


Fig. 13 Relationship between power and rotational speed

4 Conclusion

In this study, the generation of electrical energy in pressure breaker valves in an existing drinking water network in Trabzon-Karakaya was studied. Energy production was extracted from existing drinking lines in the drinking network and the performance of the energy production was quantified.

Pressure-breaking elements such as Maslak, tanks, or PBVs are used in order to break the excess pressure on the drinking water lines and reduce it to an appropriate operating pressure. By making use of the damped pressure in these facilities, the system can be used as a renewable energy source and environmentally friendly electrical energy can be obtained. An important issue is to properly design such a system to optimize its energy-producing capacity. The results are expressed as follows:

- 1.- The power obtained an hour using Pelton / varies between 0.29 kWh and 4.89 kWh. By using micro Pelton microturbines instead of 47 PBVs, a total of 84.12 kWh of electrical energy can be produced in an hour. Thus, the hourly expenditure is 0.27 kWh for each subscriber. Accordingly, the electricity needs of 311 subscribers can be met with a total energy of 84.12 kWh in the working area in one hour. To extrapolate these findings to different locations, several key factors must be taken into account. First, variations in local climate patterns, including temperature, precipitation, and seasonal changes, can significantly influence energy production efficiency. Various geographical regions may experience distinct weather conditions that can impact the performance of energy generation systems. Furthermore, the availability and characteristics of water resources, which play a vital role in the context of microturbine systems, may differ widely from one location to another. Changes in water quality, flow rates, and overall water availability can directly influence the overall performance and maintenance requirements of the system. The financial aspect is also subject to variability based on regional factors. Economic conditions, regulatory frameworks, and local market dynamics can vary sig-

- nificantly. Costs associated with installation, operation, and maintenance are contingent on regional market conditions, availability of skilled labor, and the regulatory environment governing renewable energy initiatives.
- 2.- During the design of the drinking water networks, hydraulic calculations such as pipe diameters, pressure, and microturbine costs can be analyzed, and maximum energy can be obtained by minimizing the projected costs in the new drinking water networks. Although the initial investment cost is high, it will be able to pay for itself in 3.7 years.
 - 3.- Sensors are widely used to monitor wireless water distribution systems. When the sensors are installed in places where there is no electrical power source or where battery replacement is difficult, it will be more attractive to use the energy obtained from the drinking water networks.
 - 4.- The electrical energy to be produced by placing the micromicroturbines in the appropriate places of the network lines can be integrated with electrical-power-requiring devices and savings can be achieved. Alternatively, it can be possible to charge electric vehicles at a low cost by supplying electricity to the charging stations created for electric vehicles.
 - 5.- Considering the costs of the microturbines to be used, the viability of these turbines can be assessed with a cost/benefit analysis.

4.1 Limitations

In cases where the number of revolutions is low, gearboxes are needed; while in other applications a braking system may be needed to prevent damage to the microturbine at high speeds. As discussed in this study, microturbine selection criteria can be applied according to different microturbine speeds.

4.2 Suggestion

- 1- More accurate analyzes can be obtained for the studies to be carried out by performing statistical studies with regression analysis.
- 2- Increasing the performance of microturbines; requires engineers in this field to take measures to enhance the efficiency of microturbines.

Author Contributions Conceptualization: [Veli Süme]; Methodology: [Veli Süme], [Rasoul Daneshfaraz] and [Ali Kerim]; Formal analysis and investigation: [Veli Süme], [Rasoul Daneshfaraz], [Ali Kerim], [Hamidreza Abbaszadeh] and [John Abraham]; Writing—original draft preparation: [Veli Süme], [Rasoul Daneshfaraz], [Ali Kerim] and [Hamidreza Abbaszadeh]; Writing—review and editing: [John Abraham]; Resources: [Veli Süme], [Rasoul Daneshfaraz], [Ali Kerim] and [Hamidreza Abbaszadeh]; Supervision: [Veli Süme].

Funding Open access funding provided by the Scientific and Technological Research Council of Türkiye (TÜBİTAK). The authors declare that no funds, grants, or other support were received during the preparation of this manuscript.

Data Availability Data are available from the corresponding author upon requests.

Declarations

Competing Interests The authors have no relevant financial or non-financial interests to disclose.

Open Access This article is licensed under a Creative Commons Attribution 4.0 International License, which permits use, sharing, adaptation, distribution and reproduction in any medium or format, as long as you give appropriate credit to the original author(s) and the source, provide a link to the Creative Commons licence, and indicate if changes were made. The images or other third party material in this article are included in the article's Creative Commons licence, unless indicated otherwise in a credit line to the material. If material is not included in the article's Creative Commons licence and your intended use is not permitted by statutory regulation or exceeds the permitted use, you will need to obtain permission directly from the copyright holder. To view a copy of this licence, visit <http://creativecommons.org/licenses/by/4.0/>.

References

- Abdelzaher MA (2021) Experiential investigation on the effect of heavy fuel oil substitution by high sulfur petcoke on the physico-mechanical features and microstructure of white cement composites. *Eng Res Express* 3(1):015028
- Abdelzaher MA (2022) Performance and hydration characteristic of dark white evolution (DWE) cement composites blended with clay brick powder. *Egypt J Chem* 65(8):419–427
- Abraham JP, Cheng L, Mann ME, Trenberth KE, von Schuckmann K (2022) The ocean response to climate change guides both adaptation and mitigation efforts. *Atmospheric Ocean Sci Lett* 15(4):100221
- Alnaqbi SA, Alasad S, Aljaghoub H, Alami AH, Abdelkareem MA, Olabi AG (2022) Applicability of hydropower generation and pumped hydro energy storage in the Middle East and North Africa. *Energies* 15(7):2412
- Corcoran L, Coughlan P, McNabola A (2013) Energy recovery potential using micro hydropower in water supply networks in the UK and Ireland. *Water Supply* 13(2):552–560
- Daneshfaraz R, Norouzi R, Abbaszadeh H, Kuriqi A, Di Francesco S (2022) Influence of sill on the hydraulic regime in sluice gates: an experimental and numerical analysis. *Fluids* 7(7):244
- Elkhouly HI, Abdelzaher MA, El-Kattan IM (2022) Experimental and modeling investigation of physico-mechanical properties and firing resistivity of cement pastes incorporation of micro-date seed waste. *Iran J Sci Technol Trans Civ Eng* 46:2809–2821. <https://doi.org/10.1007/s40996-021-00760-2>
- Fontana N, Giugni M, Portolano D (2012) Losses reduction and energy production in water-distribution networks. *J Water Resour Plan Manag* 138(3):237–244
- Gaius-obaseki T (2010) Hydropower opportunities in the water industry. *Int J Environ Sci* 1(3):392–402
- Itani Y, Soliman MR, Kahil M (2020) Recovering energy by hydro-turbines application in water transmission pipelines: A case study west of Saudi Arabia. *Energy* 211:118613
- Kosnik L (2010) The potential for small scale hydropower development in the US. *Energy Policy* 38(10):5512–5519
- McNabola A, Coughlan P, Williams AP (2014) Energy recovery in the water industry: an assessment of the potential of micro-hydropower. *Water Environ J* 28(2):294–304
- McNabola A, Coughlan P, Williams AP (2011) The technical and economic feasibility of energy recovery in water supply networks. In *Proceedings of International Conference on Renewable Energy and Power Quality, Las Palmas de Gran Canaria, Spain (Vol. 1315)*
- Ogayar B, Vidal PG (2009) Cost determination of the electro-mechanical equipment of a small hydro-power plant. *Renew Energy* 34(1):6–13
- Pérez-Sánchez M, Sánchez-Romero F, Ramos H, López-Jiménez P (2017) Energy recovery in existing water networks: towards greater sustainability. *Water* 9(2):97
- Postacchini M, Darvini G, Finizio F, Pelagalli L, Soldini L, Di Giuseppe E (2020) Hydropower generation through pump as turbine: Experimental study and potential application to small-scale WDN. *Water* 12(4):958
- Raihan A, Muhtasim DA, Pavel MI, Faruk O, Rahman M (2022) Dynamic impacts of economic growth, renewable energy use, urbanization, and tourism on carbon dioxide emissions in Argentina. *Environ Process* 9(2):38
- Spänhoff B (2014) Current status and future prospects of hydropower in Saxony (Germany) compared to trends in Germany, the European Union and the World. *Renew Sustain Energy Rev* 30:518–525

- Topliceanu L, Gabriel P, Furdu I (2016) Functional problems and maintenance operations of hydraulic turbines. *TEM J* 5(1):32
- Williams AA (1996) Pumps as turbines for low cost micro hydro power. *Renew Energy* 9(1–4):1227–1234
- Yazdi J, Moridi A (2018) Multi-objective differential evolution for design of cascade hydropower reservoir systems. *Water Resour Manage* 32:4779–4791

Publisher's Note Springer Nature remains neutral with regard to jurisdictional claims in published maps and institutional affiliations.